Food Science of Animal Products

Research Article

Dose-dependent structural remodeling and flavor evolution in a composite lactic acid bacteria-fermented whole-egg beverage: integrated physicochemical, structural and flavor analyses

Danrong Yu[§], Yaping Shen[§], Ni Zhang, Yutong Han, Bohan Wang, Xiaoyu Zhang, Ling Ma ✉, Zhihui Yu ✉

College of Food Science and Engineering, Shanxi Agricultural University, Jinzhong 030801, China

[§] These authors contributed equally to this work.

✉ Address correspondence to Ling Ma, ml0359@163.com; Zhihui Yu, zhihuisxau@163.com

Received: March 19, 2026; Revised: April 7, 2026; Accepted: April 29, 2026

Abstract: Whole egg is a nutrient-dense matrix, yet its application in beverages is often constrained by poor colloidal stability and "eggy" off-flavor. This study elucidated dose-dependent effects of mixed lactic acid bacteria inoculation on the physicochemical properties, protein structural evolution, and flavor quality of a fermented whole-egg beverage (WEB). A 1:1 (*V*/*V*) mixture of *L. delbrueckii* subsp. *bulgaricus* and *Streptococcus thermophilus* (total viable count: (1.1 ± 0.1) × 10^9 CFU/mL) was inoculated into pasteurized whole egg beverage matrix at 0%, 1%, 3%, 5% and 7% (*V*/*V*), corresponding to groups WE, FWE-1%, FWE-3%, FWE-5% and FWE-7%. Fermentation proceeded at 42 °C for 4 h, followed by 36 h ripening at 4 °C. All samples were characterized using dispersion metrics, spectroscopy, electrophoresis, *in vitro* digestion, gas chromatography-ion mobility spectrometry, electronic nose, electronic tongue, and sensory evaluation. Fermentation acidified WEB, to pH 4.15–4.36, decreased relative turbidity (normalized to the control), and improved dispersion uniformity (minimum polydispersity index was 0.305 at 7%). Soluble protein content increased to 10.24–12.27 mg/g (*vs.* 2.53 mg/g in the control), and antioxidant capacity was enhanced, with 1,1-diphenyl-2-picrylhydrazyl radical and 2,2′-azino-bis(3-ethylbenzothiazoline-6-sulfonic acid) cation radical scavenging rates reaching 95.84% (FWE-5% group) and 82.14% (FWE-7% group), respectively. Second-derivative ultraviolet, intrinsic fluorescence, and Fourier transform infrared spectroscopy amide I redshift indicated protein conformational remodeling, supported by sodium dodecyl sulfate-polyacrylamide gel electrophoresis showing progressive degradation of high-molecular-weight subunits. These changes improved nutritional functionality, with *in vitro* protein digestibility maximized at 3% inoculation. Flavor analyses revealed fermentation-driven reconfiguration of volatile and taste profiles, including aroma enrichment and reduced bitterness. Sensory results identified 3% inoculation as optimal, delivering the highest overall acceptability with balanced sourness and diminished eggy odor. This research provides a scientific basis for optimizing inoculation levels in fermented WEB and offers new perspectives for the development of functional egg-based fermented products.

Keywords: whole-egg beverages; composite lactic acid bacteria fermentation; antioxidant activity; protein conformation; volatile profile; sensory evaluation

Citation: D. R. Yu, Y. P. Shen, N. Zhang, et al., Dose-dependent structural remodeling and flavor evolution in a composite lactic acid bacteria-fermented whole-egg beverage: integrated physicochemical, structural and flavor analyses, Food Sci. Anim. Prod. 4 (2026) 9240176. https://doi.org/10.26599/FSAP.2026.9240176.

1 Introduction

Eggs are a nutrient-dense food, offering high-quality protein, lipids, vitamins (A, B, D, E), and essential minerals (Ca, P, K, Fe, Zn). Their high nutritional density and excellent digestibility have established them as a superior protein source[1]. From a nutritional perspective, the essential amino acid profile and bioavailability of egg white proteins are comparable to those of milk proteins. Additionally, yolk components such as phospholipids and carotenoids provide benefits related to neurodevelopment, lipid metabolism, and antioxidant defense[2]. Despite these advantages, egg processing faces two major constraints: limited flavor diversity and a high cholesterol content[3]. The higher fat and cholesterol levels in yolk raise health concerns, especially for patients with cardiovascular disease[4]. Moreover, deep processing of eggs remains underdeveloped. Current products focus largely on fresh eggs, salted eggs, preserved eggs, and primary ingredients such as egg white or yolk powders. These forms limit the high-value utilization of egg resources. Whole egg beverages (WEB), which are typically prepared from liquid whole egg, offer a nutrient-rich matrix and a distinctive taste. However, their relatively high cholesterol and triglyceride contents limit their market potential as a health food[5]. Therefore, the development of low-cholesterol WEB has become an important direction for new product development.

Lactic acid bacteria (LAB) fermentation technology can improve the flavor and nutritional attributes of egg products through pH reduction, organic acid accumulation, and enhanced proteolysis[6]. Probiotic strains may also lower cholesterol through multiple mechanisms, including bile salt deconjugation by bile salt hydrolase (BSH), short-chain fatty acid production, cholesterol assimilation into cell membranes, and conversion of cholesterol to coprostanol, which has a lower intestinal absorption rate[7]. Several studies have further shown that BSH-active *Lactobacillus* strains can upregulate hepatic cytochrome P450 family 7 subfamily A member 1 via the

farnesoid X receptor pathway, which accelerates cholesterol catabolism to bile acids[8]. In dairy (e.g., yogurt) fermentations, starter cultures such as *Streptococcus thermophilus* and *Lactobacillus bulgaricus* convert lactose to lactic acid and generate aroma-active metabolites, including diacetyl and ethyl acetate, which contribute fresh dairy notes and mild acidity[9]. Fermentation also promotes protein reorganization and network formation, which supports a smooth texture and stable gel structure[2]. These observations highlight the potential of LAB fermentation for the development of functional foods with improved sensory quality and lipid-related health attributes.

In recent years, egg-based fermented yogurt alternatives, prepared from liquid whole egg or egg white, have been proposed to obtain yogurt-like texture and sensory properties through LAB fermentation. Evidence indicates that egg components provide a favorable matrix for LAB growth and can yield desirable gel strength, emulsification stability, and sensory quality. However, previous studies have primarily examined the effects of fermentation on egg protein functionality[10–11]. A comprehensive understanding of how the key parameters of the fermentation process—particularly the inoculum dose—systematically regulate the physicochemical properties, protein conformation, and flavor quality of whole-egg fermented beverages remains lacking. The inoculum dose determines the initial microbial load and metabolic intensity, and thus represents a critical variable that controls acidification, texture development, and flavor formation. However, the dose-response relationship between the inoculum level and the molecular structure and colloidal stability of proteins in the whole-egg matrix remains unclear.

In this study, liquid whole egg served as the main substrate and was supplemented with milk and stabilizers to prepare a fermented WEB using a composite LAB starter. We investigated the effects of inoculation levels (0%, 1%, 3%, 5%, and 7%, *V*/*V*) on pH, zeta potential, particle size distribution, and protein higher-order structure, as characterized by ultraviolet (UV) absorption, intrinsic fluorescence, and surface hydrophobicity, etc. of the product. A multidimensional flavor evaluation framework was further applied, including gas chromatography-ion mobility spectrometry (GC-IMS), electronic nose, electronic tongue, and sensory evaluation, to assess product quality from microstructural and sensory perspectives. This work aims to clarify how inoculum dose regulates protein conformational evolution and flavor development in fermented WEB, thereby providing a basis for process optimization and product development.

2 Materials and methods

2.1 Materials

Fresh eggs, sterilized milk, and granulated sugar were purchased from Shanxi Jiayuan Supermarket (Jinzhong, China). The mixed bacterial culture (*Lactobacillus delbrueckii* subsp. *bulgaricus* and *S. thermophilus*) was provided by the Dairy Products Laboratory at Shanxi Agricultural University. Sodium carboxymethyl cellulose (CMC-Na) and guar gum were provided by Shandong Chengyu Biotechnology Co., Ltd. (Tai'an, China). Nile red, fluorescein isothiocyanate (FITC), 2,4,6-tripyridyl-*s*-triazine (TPTZ), 1,1-diphenyl-2-picrylhydrazyl (DPPH), 2,2′-azino-bis(3-ethylbenzothiazoline-6-sulfonic acid) reagents, and biochemical reagents such as Folin-Ciocalteu reagent, chymotrypsin, trypsin, and alkaline protease were purchased from Aladdin Reagents (Shanghai) Co., Ltd. (Shanghai, China).

2.2 Preparation of fermented WEB

Fresh eggs were washed, and shells were disinfected with 75% (*V*/*V*) ethanol. Eggs were cracked, homogenized manually using a hand-held blender for 2 min, and filtered through four layers of cheesecloth. The filtrate was pasteurized in a water bath at 58.8 °C for 5 min and then cooled to room temperature. The egg mixture (10%, *V*/*V*), milk (8%, *V*/*V*), sucrose (6 g/100 mL), and purified water (74%, *V*/*V*) were mixed thoroughly. A composite stabilizer (0.3 g/100 mL; CMC-Na:guar gum = 5:1, *m*/*m*) was added, and the mixture was stirred in a 60 °C water bath until fully dissolved. Viable counts of the starter strains were determined by the pour-plate method: *L. delbrueckii* subsp. *bulgaricus* was counted on MRS agar, yielding $(1.0 \pm 0.1) \times 10^9$ CFU/mL, while *S. thermophilus* was counted on M17 agar, yielding $(1.2 \pm 0.1) \times 10^9$ CFU/mL. After blending the two strains at a 1:1 (*V*/*V*) ratio, the composite starter culture exhibited a total viable density of $(1.1 \pm 0.1) \times 10^9$ CFU/mL. This mixed starter (1:1, *V*/*V*) was then inoculated into the pasteurized whole-egg matrix at 1%, 3%, 5%, or 7% (*V*/*V*) of the total volume, corresponding to initial cell loads in the beverage of approximately 1.1×10^7, 3.3×10^7, 5.5×10^7, and 7.7×10^7 CFU/mL, respectively; an uninoculated sample served as the control group (WE, 0%), and the five groups were denoted as WE (0%), FWE-1%, FWE-3%, FWE-5%, and FWE-7%. Fermentation was conducted at 42 °C for 4 h, followed by ripening at 4 °C for 36 h. After ripening, the fermented samples were divided into two portions: one was stored at 4 °C, and the other was freeze-dried using a Freezone 4.5L lyophilizer (Labconco, Kansas City, MO, USA). The freeze-dried powders were immediately sealed and stored at 4 °C in the dark for long-term preservation.

The samples for determination of intrinsic fluorescence spectra, surface hydrophobicity, and *in vitro* protein digestibility (IVPD) are freeze-dried powders, while beverages are used as samples unless otherwise specified.

2.3 Determination of color

After calibration with a standard black and white tile, the brightness value (L^*), redness value (a^*), and yellowness value (b^*) were measured using a colorimeter (CR-400, Konica Minolta, Tokyo, Japan). Measurements were performed in triplicate[12].

2.4 Determination of pH

Samples (10 mL) were collected at 0, 10, 20, 30, and 40 h during ripening. The pH was measured with a calibrated pH meter (PHB-4, Mettler-Toledo, Zurich, Switzerland) at 20–22 °C.

2.5 Determination of zeta potential and average particle size

Each sample (1 mL) was diluted 100-fold with phosphate buffered saline (PBS), filtered through a 0.45 μm syringe filter, and transferred to a disposable cuvette (0.75 mL). Zeta potential, particle size and polydispersity index (PDI) were measured using a Zetasizer Nano ZS90 (Malvern Instruments, Malvern, UK)[13].

2.6 Determination of turbidity

Samples were mixed thoroughly, and absorbance was measured at 860 nm using a UV-Vis spectrophotometer (TU-1901, Beijing Puxi General Technology Co., Ltd., Beijing, China). Turbidity was expressed as absorbance at 860 nm ($A_{860\,nm}$).

2.7 Stability evaluation

The stability of the post-mature samples (0–40 h) was evaluated using a centrifugation precipitation method. Samples (10 mL) were weighed (m, g), centrifuged at 6 500 r/min for 20 min, and the supernatant was discarded. The precipitate was weighed (W, g). The precipitation rate was calculated using a standard formula, with three parallel replicates for each group[14]. The precipitation rate was calculated as formula (1):

$$\text{Precipitation rate}\ (\%) = \frac{W}{m} \times 100 \quad (1)$$

2.8 Determination of soluble protein content

Soluble protein content was determined by the Bradford method. Samples were diluted 100-fold; 100 μL of diluted sample was mixed with 5 mL of Coomassie brilliant blue G250 reagent (0.05 g/100 mL in 95% ethanol and 85% phosphoric acid). After mixing and brief incubation, absorbance was measured at 595 nm. Soluble protein content was calculated from a calibration curve[15].

2.9 Determination of UV spectra

The sample was diluted 100-fold in PBS and scanned from 230 to 400 nm using a UV-Vis spectrophotometer (U1901PC, Beijing Puxi General Technology Co., Ltd., Beijing, China). Spectra were recorded with a 2 nm bandwidth and 1 nm intervals. Three replicates were averaged, and the second-derivative spectra were calculated[16].

2.10 Determination of intrinsic fluorescence spectra

Lyophilized samples were reconstituted to 0.1 mg/mL. Fluorescence spectra were recorded using a spectrofluorometer (RF-5301, Shimadzu, Kyoto, Japan) with excitation at 295 nm and emission scanned from 310 to 450 nm (scan rate: 1 200 nm/min; slit width: 5 nm).

2.11 Determination of surface hydrophobicity

Lyophilized samples were dissolved to 1 mg/mL. Sample solution (1 mL) was mixed with 200 μL bromophenol blue (BPB, 1 mg/mL). After incubation at 25 °C for 10 min, samples were centrifuged at 2 000 r/min for 15 min at 4 °C. The supernatant was diluted 10-fold, and absorbance was measured at 595 nm. PBS was used as the blank[17]. Surface hydrophobicity was expressed as the binding amount of BPB, and was calculated as formula (2):

$$\text{Surface hydrophobicity}\ (\mu g) = \frac{A_{\text{Blank}} - A_{\text{Sample}}}{A_{\text{Blank}}} \times 200\ \mu g \quad (2)$$

2.12 Determination of Fourier transform infrared (FTIR) spectroscopy

Samples (1 mg) were mixed with KBr, ground, and pressed into pellets. FTIR spectra were collected using a spectrometer (TENSOR27, Bruker, Germany) from 500 to 4 000 cm^{-1} (resolution 4 cm^{-1}). Each sample was measured in triplicate.

2.13 Confocal laser scanning microscopy (CLSM) observation

Samples (0.5 mL) were mixed with 50 μL of dye solution containing Nile red and FITC (1 mg/mL each; 1:1, V/V). After incubation in the dark at room temperature overnight, samples were observed using a CLSM (Olympus FV1200, Tokyo, Japan). Lipids were imaged at 568 nm/600 nm (excitation wavelength/emission wavelength), and proteins at 488 nm/520 nm. Images were acquired at 10× magnification[18].

2.14 Sodium dodecyl sulfate-polyacrylamide gel electrophoresis (SDS-PAGE)

SDS-PAGE was performed using 12% resolving and 4% stacking gels. Samples were denatured for 5 min, centrifuged at 8 000 × g for 5 min, and 10 μL of the supernatant was loaded. Electrophoresis was conducted at 90 V for 30 min and then at 110 V for 90 min. Gels were stained with Coomassie brilliant blue R250 for 1 h, destained with deionized water for 12 h, and imaged[19].

2.15 Determination of antioxidant capacity

Samples ((2.0 ± 0.1) g) were extracted with 20 mL of methanol by vortexing for 5 min, then centrifuged at 5 000 × g for 10 min at 4 °C, and the supernatant was collected. Three independent replicates were performed for each assay. The DPPH assay, the ABTS assay, and the ferric reducing antioxidant power (FRAP) assay were performed according to the methods described in references[20–22] with slight modifications. For the DPPH assay, a 100 μL aliquot of sample extract was mixed with 3.9 mL of DPPH solution (60 μmol/L prepared in methanol) and incubated in the dark at room temperature for 30 min, after which absorbance was measured at 515 nm[20]. For the ABTS assay, a working solution was prepared by mixing ABTS (7 mmol/L) and potassium persulfate (2.45 mmol/L) in a 1:1 (V/V) ratio and incubating in the dark for 12–16 h at room temperature; the solution was diluted with ethanol to an absorbance of 0.70 ± 0.02 at 734 nm. A 20 μL aliquot of sample extract was mixed with 180 μL of the ABTS working solution in a 96-well plate and incubated in the dark for 6 min, and absorbance was measured at 734 nm[21]. For the FRAP assay, the FRAP working reagent was prepared fresh by mixing 300 mmol/L acetate buffer (pH 3.6), 10 mmol/L TPTZ in 40 mmol/L HCl, and 20 mmol/L $FeCl_3$ in a 10:1:1 (V/V) ratio. A 200 μL aliquot of sample extract was mixed with 1.8 mL of FRAP reagent and incubated at 37 °C for 30 min in the dark; the absorbance of the formed Fe^{2+}-TPTZ complex was measured at 593 nm[22]. Results were calculated using a $FeSO_4$ standard curve and expressed as millimolar Fe^{2+} equivalents.

2.16 Determination of IVPD

IVPD was determined using a multi-enzyme system (31 mg chymotrypsin, 16 mg trypsin, and 13 mg alkaline protease dissolved in 10 mL of water, pH 8.00 ± 0.05). Lyophilized powder (2.5 mg) was dissolved in 10 mL water and incubated at 37 °C for 1 h. The pH was adjusted to 8.0, 1 mL enzyme solution was added, and the pH change after 10 min was recorded[23]. IVPD was calculated as formula (3):

$$\text{IVPD}\,(\%) = 65.6 + 18.10 \times \Delta pH_{10\ \text{min}} \quad (3)$$

Where $\Delta pH_{10\ \text{min}}$ is the change in pH from 8.00 to the value after 10 min of hydrolysis.

2.17 GC-IMS analysis

Volatile compounds were analyzed using headspace GC-IMS (FlavourSpec, G.A.S., Dortmund, Germany). Fresh samples ((4.00 ± 0.01) g) was placed into a 20 mL headspace vial and

incubated at 60 °C for 20 min with agitation (500 r/min). A 500 μL aliquot of headspace gas was injected using a heated syringe (80 °C) in split injection mode. Separation was performed on an MXT-WAX column (30 m × 0.53 mm, 1 μm) at 60 °C. Nitrogen (≥ 99.99%) served as carrier gas with the following program: 2 mL/min for 2 min, ramp to 100 mL/min over 18 min, and hold for 10 min. The drift tube temperature was 45 °C, with a drift gas flow of 150 mL/min. Ionization used a tritium source (^{3}H, 110 MBq) at 5 kV (≈ 500 V/cm). For identification, *n*-ketones (C_4–C_9) were used to calculate retention index (RI). Compounds were assigned by matching drift time and RI against the GC-IMS NIST library.

2.18 Electronic nose analysis

An electronic nose (PEN3, Airsense Analytics, Schwerin, Germany) was used. Sample (3.0 mL) was diluted to 25 mL with water, and 5 mL was transferred to a sealed headspace vial. Sensors were cleaned for 240 s and zeroed for 10 s. The injection flow rate was 300 mL/min, and acquisition time was 90 s. The PEN3 electronic nose system was equipped with a sensor array of 10 metal oxide semiconductor sensors, each sensitive to different volatile compounds: W1C: aromatic, W5S: broad-range, W3C: aromatic, W6S: hydrogen, W5C: aromatic aliphatics, W1S: broad, W1W: organic sulfur, W2S: alcohol, W2W: sulfur chlorinated, and W3S: methane aliphatics.

2.19 Electronic tongue analysis

Samples (10 mL) were placed in dedicated vials for an electronic tongue (SA402B, Beijing Ensoft Technology Co., Ltd., Beijing, China). Sensors were rinsed in cleaning solution (90 s) and reference solution (120 s × 2). After a 30 s stabilization period, measurements were recorded for 30 s. Sensors C00, AE1, CA0, CT0, and AAE were tested in four cycles; the first cycle was discarded, and the mean of the remaining three cycles was used.

2.20 Sensory evaluation

This study strictly adhered to ethical standards. All participants signed written informed consent forms, confirming their right to withdraw at any time without penalty. Prior to evaluation, each panelist received comprehensive disclosure regarding the study's requirements, procedures, and potential risks, including allergen information for eggs and dairy. The protocol was reviewed by the Ethics Committee of Shanxi Agricultural University. Because the study involved only sensory evaluation of commercially available edible products and no invasive procedures, it met the criteria for ethical exemption according to institutional guidance. Fifteen food science students (8 females and 7 males; aged 22–26 years) were recruited as panelists. All participants underwent preliminary screening and a two-week systematic training program covering basic taste identification, intensity scaling, and product characteristic familiarization. After meeting repeatability and consistency criteria, the final evaluation panel was established. According to ISO 8586:2023, a minimum of 8–12 trained panelists is generally acceptable for descriptive sensory analysis; thus, our panel of 15 trained panelists meets the recommended requirement. To minimize positional and carryover effects, samples were presented to each panelist in a randomized order, and the serving sequence was balanced across sessions. A structured scale was used for the evaluation. Five key sensory attributes were defined for the fermented WEB samples: color (uniformity and typicality), odor (fermented aroma intensity and absence of off-odors), texture (smoothness and velvety mouthfeel), taste (sweet-sour balance, bitterness/astringency, and aftertaste), and overall acceptability. Attributes were scored on a 10-point scale (1 = extremely low/unacceptable; 10 = extremely high/highly preferred). The sensory evaluation methodology was designed and implemented in accordance with relevant ISO guidelines (ISO 8586:2023; ISO 6658:2017) to ensure procedural standardization and result reliability. Personal identifying information collected during the informed consent process (e.g., names and signatures) was stored securely and is not disclosed in this manuscript, ensuring participants' privacy and confidentiality in compliance with applicable data protection standards.

2.21 Statistical analysis

All measurements were performed in triplicate, and results are expressed as mean ± standard deviation. Differences among groups were analyzed using one-way analysis of variance followed by Duncan's multiple range test ($P < 0.05$). Multivariate analyses (principal component analysis (PCA) and partial least squares discriminant analysis (PLS-DA)) were used to visualize group separation. Hierarchical clustering and heatmaps were generated based on the signal intensities of key volatiles.

3 Results and discussion

3.1 Effect of inoculation level on the color of WEB

Fermentation significantly altered the color profile of the WEB (Table 1). The WE group showed a significantly lower L^* (31.88) compared to all FWE groups ($P < 0.05$), indicating that fermentation effectively enhanced the apparent brightness of the product. This improvement was primarily attributed to the degradation of macromolecular proteins by proteases secreted by LAB, which reduced the particle size. According to Mie scattering theory, smaller particles exhibit higher scattering efficiency for visible light, thereby enhancing the perceived brightness[24]. The absolute a^* of the FWE groups showed a decreasing trend with the inoculum level increased compared to WE group, indicating a shift in color towards a more neutral tone. The organic acids produced

Table 1 Effect of fermentation on the color of WEB.

Group	L^*	a^*	b^*
WE	31.88 ± 0.21^b	0.41 ± 0.01^c	3.59 ± 0.08^c
FWE-1%	64.34 ± 0.26^a	0.03 ± 0.00^b	15.82 ± 0.15^a
FWE-3%	63.79 ± 0.38^a	0.07 ± 0.01^a	15.70 ± 0.34^a
FWE-5%	64.18 ± 0.54^a	−0.12 ± 0.01^d	15.32 ± 0.08^b
FWE-7%	63.73 ± 0.26^a	−0.09 ± 0.01^c	15.21 ± 0.09^b

Note: Different lowercase letters in the same column represent significant differences at $P < 0.05$.

during fermentation significantly lowered the system's pH, which in turn affected the charge state and dispersibility of yolk carotenoids. The acidic environment likely induced partial degradation or conformational changes in the carotenoids, thereby reducing their color-contributing effect[25]. The b^* showed an initial increase followed by a decrease with the inoculum level increased compared to WE group. The b^* of all FWE groups were significantly higher than that of the WE group (3.59). At low inoculation levels (1%–3%), fermentation likely promoted the synthesis and release of yellow metabolites, such as carotenoid derivatives. In contrast, at high inoculation levels (5%–7%), excessive acidification destabilized the carotenoids, leading to a subsequent decline in the b^*[26–27]. In summary, fermentation synergistically improved the color of WEB through protein degradation-enhanced light scattering (increased L^*) and pH regulation-metabolite synthesis (changes in a^* and b^*).

3.2 Effect of inoculation level on the pH of WEB during ripening

During the ripening period, the pH of the WE group remained relatively stable (7.74–8.21), whereas the pH of all FWE groups were significantly lower than that of the WE group. As ripening progressed, the pH of the FWE groups showed an overall downward trend, eventually decreasing to 4.15–4.36 (Figure 1A). This decline was attributed to the continuous accumulation of organic acids, primarily lactic acid and acetic acid, produced by LAB metabolizing lactose and sucrose[28]. The pH decline kinetics exhibited a distinct two-phase pattern. In the early ripening stage (0–20 h), the acidification rate was the fastest, as the microorganisms were in the logarithmic growth phase and actively produced acids. During the mid-to-late stage (20–40 h), acidification entered a plateau phase, and no significant differences in pH were observed among the inoculated groups. Notably, after 40 h of ripening, the pH of the FWE-1% group (4.15) was significantly lower than that of the FWE-3% (4.36), FWE-5% (4.33), and FWE-7% (4.30) groups, while no significant difference existed among the latter three groups. A plausible explanation is that high inoculum levels intensify competition for nutrients and space, which can shorten the exponential phase and reduce net acid production during the late stage. In contrast, a lower inoculum level may sustain active growth for longer, supporting continued acid production[29].

3.3 Effect of inoculation level on the zeta potential and average particle size of WEB

Zeta potential analysis (Figure 1B) revealed that compared to the WE group (–6.54 mV), the absolute zeta potential values of the FWE-1%, FWE-5%, and FWE-7% groups increased significantly ($P < 0.05$), with the FWE-7% group reaching the maximum absolute value (13.93 mV). Only the FWE-3% group (–6.21 mV) showed no significant difference from the WE group. This was because the 3% inoculation level resulted in moderate organic-acid production, which caused a slight decline in system pH that remained well above the isoelectric point of major egg/milk proteins around 4.6–4.7. As a result, the surface charges of the protein particles were neither substantially neutralized nor redistributed. Meanwhile, the gentle proteolytic activity derived from LAB avoided the excessive hydrolysis-driven exposure of

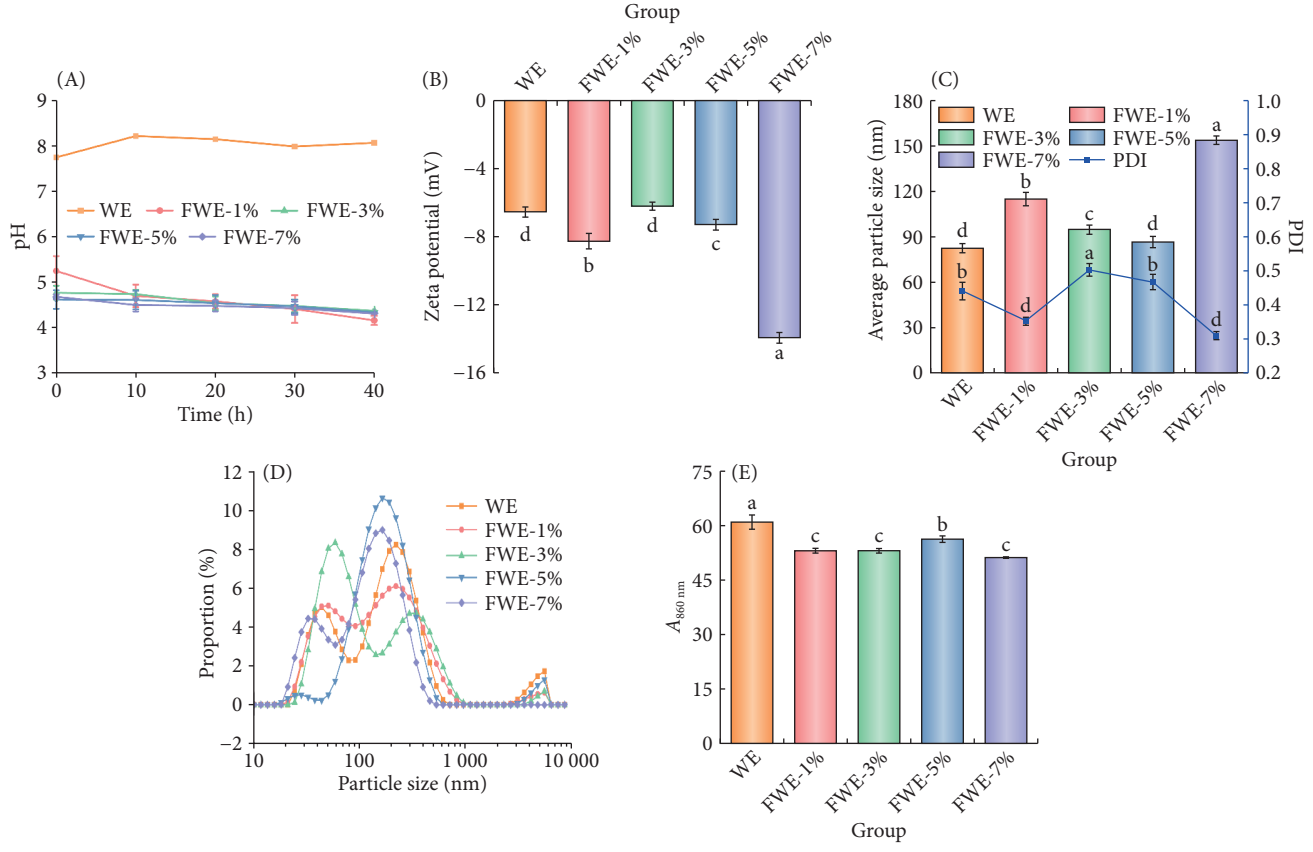

Figure 1 Effect of inoculation level on the (A) pH, (B) zeta potential, (C) average particle size and PDI, (D) particle distribution, and (E) turbidity of WEB. Different lowercase letters represent significant differences at $P < 0.05$.

negatively charged residues seen in the FWE-5% and FWE-7% groups as well as the localized acidification heterogeneity found in the FWE-1% group, allowing the FWE-3% system to preserve a near-native protein architecture while accumulating appreciable flavor-active metabolites. Increased absolute zeta potential indicated enhanced surface charge density on the particles, which stemmed from two synergistic fermentation effects. LAB metabolism generated organic acids that altered the system pH and ionic environment, while protease hydrolysis exposed more charged amino acid residues such as aspartic and glutamic acids. These two effects worked together to strengthen electrostatic repulsion between particle surfaces, preventing particle approach and aggregation to effectively inhibit sedimentation and improve system stability[30]. Furthermore, lactic acid produced during fermentation lowered the system pH. As the pH approached the isoelectric point of casein between 4.6 and 4.7, partial protein aggregation occurred due to charge neutralization, forming a gel network. However, fermentation in the FWE-7% group enhanced electrostatic repulsion through a charge-density compensation mechanism, delaying sedimentation formation[31]. Particle size analysis results (Figures 1C and D) showed a significant increase in the particle size distribution of the FWE groups within the 10–1 000 nm range. Among them, the FWE-3% group had the highest proportion of particles in the 10–100 nm range, while the FWE-7% group exhibited a bimodal distribution. The average particle size of the FWE-5% group (86.53 nm) was closest to that of the WE group (82.56 nm), whereas the FWE-7% group had the largest average particle size (153.90 nm). Regarding the PDI, the FWE-7% group (0.31) showed a 24.39% reduction compared to the WE group (0.44), indicating that high inoculum fermentation, despite increasing the average particle size (likely due to rearrangement of protein-lipid aggregates), significantly improved the uniformity of particle size distribution[32]. This is because, under high inoculum conditions, proteases hydrolyzed the heterogeneous macromolecular protein aggregates more thoroughly, generating more uniformly sized nanoparticles[33]. The bimodal distribution observed in the FWE-7% group can be attributed to the formation of two distinct colloidal particle populations during fermentation: the small-particle peak corresponds to low-molecular-weight peptides and protein fragments produced by enzymatic hydrolysis, while the large-particle peak likely originates from casein-based gel microparticles formed near the isoelectric point[34].

3.4 Effect of inoculation level on the turbidity of WEB

As shown in Figure 1E, fermentation with compound strains significantly reduced the turbidity of the WEB ($P < 0.05$). The WE group exhibited the highest turbidity (60.94%), whereas the turbidity of the FWE groups decreased significantly overall. Among them, no significant difference ($P > 0.05$) was observed between the FWE-1%, FWE-3%, and FWE-7% groups, while the FWE-5% group (56.16%) showed significantly higher turbidity than the other inoculated groups ($P < 0.05$). The primary mechanism for turbidity reduction is the degradation and reconstruction of light-scattering particles by the protease system of LAB. When particles or aggregates larger than 0.1 μm are present in the beverage system, they cause light refraction and scattering, resulting in a cloudy appearance[35]. The turbidity of whole-egg liquid mainly originates from the colloidal dispersions formed by globular proteins, such as ovalbumin (~45 kDa), ovotransferrin (~78 kDa), and ovomucin (~28 kDa), in the aqueous phase. The protease system of LAB consists of extracellular proteases and intracellular peptidases. Extracellular proteases degrade proteins into oligopeptides, which intracellular peptidases further hydrolyze into low molecular weight peptides and free amino acids[6]. Therefore, when proteins are hydrolyzed from large aggregates into nanosized small peptides, the single-particle scattering cross-section decreases sharply, leading to a significant reduction in the macroscopic turbidity of the system[36]. The abnormally high turbidity observed in the FWE-5% group deserves attention. Combined with pH data analysis, the rapid pH decline during fermentation in this group may have approached the isoelectric point region of whole-egg proteins within a short time. The competition between "turbidity reduction via enzymatic hydrolysis" and "turbidity increase due to isoelectric aggregation" likely resulted in the higher final turbidity in the FWE-5% group compared to the other inoculation groups. In contrast, the FWE-7% group exhibited stronger protease activity and more thorough hydrolysis, where the reduction of the scattering cross-section by small peptides became the dominant factor, allowing the turbidity to return to a level comparable to that of the low-inoculation groups.

3.5 Effect of inoculation level on the stability of WEB during ripening

As shown in Figure 2A, the precipitation rate in the WE group initially decreased and then gradually increased as ripening proceeded, while the precipitation rates of the FWE groups followed a generally declining trend and eventually stabilized. During the early ripening period (0–10 h), the precipitation rate in the FWE groups was significantly higher than that in the WE group ($P < 0.05$). However, by 40 h, the precipitation rates of FWE-1% (21.01%) and FWE-3% (21.30%) fell below that of the WE group (22.25%). Over the entire process, fluctuations in the FWE-1% and FWE-3% groups were significantly lower than those in the FWE-5% and FWE-7% groups ($P < 0.05$). FWE-5% exhibited the highest precipitation rate throughout (25.71%–40.87%), significantly exceeding all other groups ($P < 0.05$), indicating a negative effect of high inoculum on long-term system stability. This phenomenon may relate to a shift in the substrate equilibrium. When the inoculum exceeded 3%, the rapid proliferation of LAB accelerated nutrient consumption. Excessive lactic acid production induced a marked pH decline, which approached the isoelectric point of casein (pH ≈ 4.6). As pH neared this point, electrostatic repulsion between protein molecules weakened, hydrophobic interactions increased, leading to the contraction of the colloidal network and enhanced syneresis. Excessive whey separation, and thus poorer stability, occurred in groups with higher inocula[37]. In the later ripening stage (e.g., 40 h), the precipitation rate of FWE-5% sometimes dropped below that of the control (WE) group. This may be explained by the excessively acidic environment (very low pH) inhibiting subsequent metabolic activity of LAB, which could moderate protein aggregation caused by over-acidification. Moreover, the high early acidity also suppressed further bacterial proliferation, slowing the subsequent acidification rate and thereby reducing whey separation in the later phase[38].

3.6 Effect of inoculation level on the surface soluble protein content of WEB

The soluble protein content of the FWE groups (10.24–12.27 mg/g) was significantly higher than that of the WE group (2.53 mg/g), approximately 4.5-fold greater ($P < 0.05$) (Figure 2B). This substantial increase primarily resulted from the stepwise hydrolysis

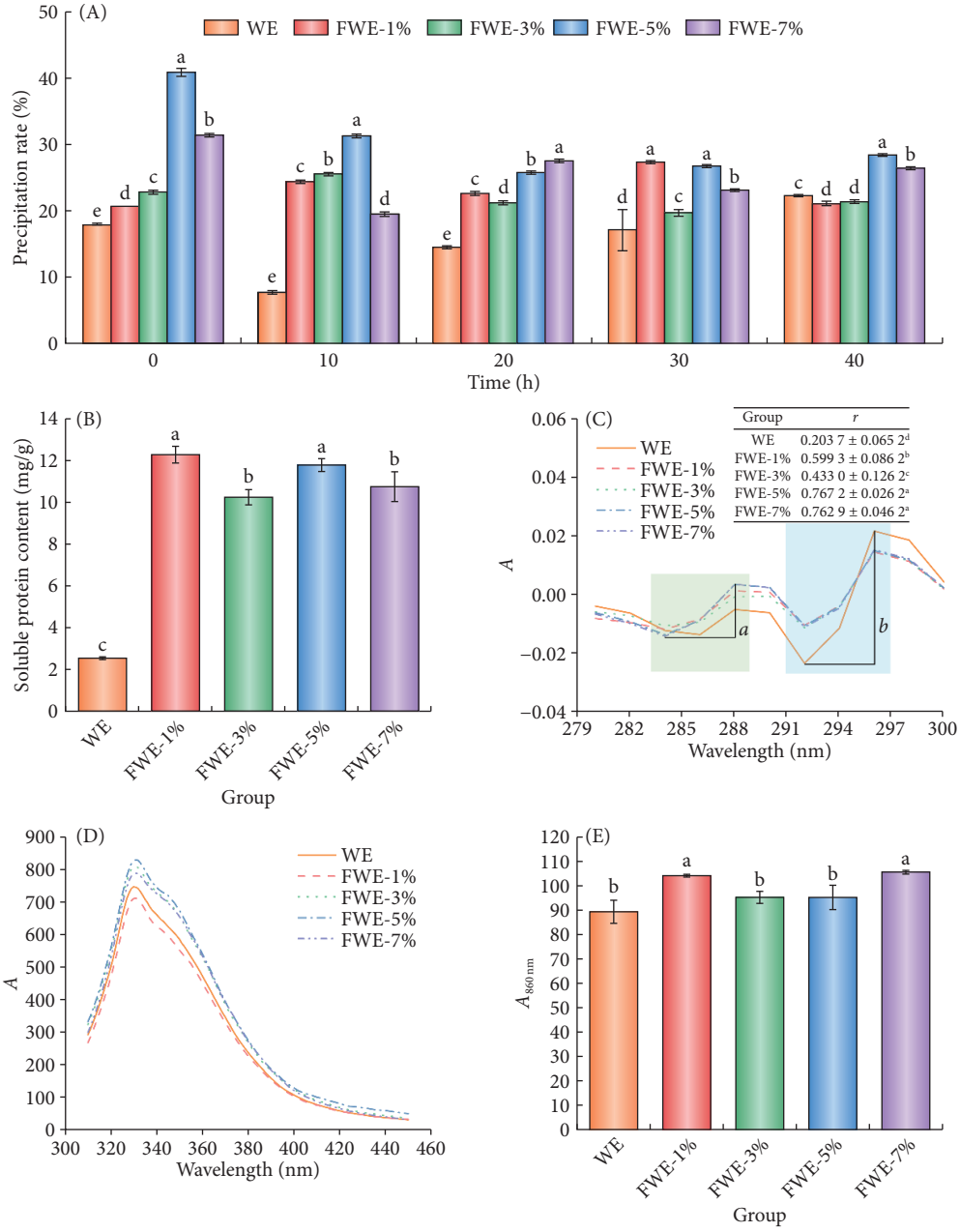

Figure 2 Effect of inoculation level on the (A) stability, (B) soluble protein content, (C) second derivative UV spectra, (D) endogenous fluorescence UV spectra, and (E) surface hydrophbicity of WEB. Different lowercase letters represent significant differences at $P < 0.05$.

of whole-egg macromolecular protein by the protease system of LAB[39]. In the early fermentation stage, endogenous proteases drove the initial hydrolysis. Subsequently, the microbial enzyme system enhanced protein hydrolysis sensitivity by altering the conformation of amino acid residues and the spatial structure of polypeptide chains, thereby increasing the soluble protein content[40]. Furthermore, the pH decrease induced by fermentation shifted the system away from the isoelectric point of the proteins, increasing their net charge and solubility, and further promoted the release of soluble proteins. Notably, the effect of different inoculation concentrations on protein content showed a gradient. FWE-1% (12.27 mg/g) and FWE-5% (11.78 mg/g) had relatively high levels with no significant difference ($P > 0.05$), whereas FWE-3% (10.24 mg/g) and FWE-7% (10.74 mg/g) exhibited lower contents. This phenomenon reflects the complexity of the dynamic "substrate-enzyme-product" balance in microbial fermentation systems. An excessively high inoculum may reduce proteolytic efficiency due to mechanisms such as intensified nutrient competition among cells, accumulation of organic acids that inhibit protease activity at optimal pH, or feedback inhibition by hydrolysis products, deviating the system from its optimal enzymatic efficiency[41].

3.7 Effect of inoculation level on the second derivative UV spectra of WEB

The second-derivative UV spectra (Figure 2C) displayed a double-peak (288, 296 nm) and double-trough (283, 292 nm) pattern in the 282–297 nm range. The peak at 288 nm was attributed to the combined effects of tyrosine (Tyr) and tryptophan (Trp) residues[42]. Changes in the microenvironment of Tyr residues

can be characterized by the amplitude ratio (r, where $r = a/b$, defined as the ratio of the distance between positive and negative absorption peaks and troughs). A higher r value typically indicates that Tyr residues, which were originally buried, become more exposed to the surface and undergo relocation toward hydrophobic regions and changes in three-dimensional positioning as the protein structure depolymerizes and unfolds during hydrolysis. In contrast, the r value for Trp shows less correlation with solvent polarity[43]. The r value of the WE group (0.203 7) was significantly lower than that of all FWE groups ($P < 0.05$) (Figure 2C). FWE-5% (0.767 2) and FWE-7% (0.762 9) exhibited significantly higher r values than FWE-1% and FWE-3% ($P < 0.05$), and FWE-1% (0.599 3) was significantly higher than FWE-3% (0.433 0) ($P < 0.05$). The significant increase in r values in the high-inoculum groups indicates that extensive proteolysis during fermentation induced substantial unfolding of the tertiary structure of whole-egg proteins, exposing Tyr residues originally buried in hydrophobic cores to the polar solvent. This result aligns with findings reported by Chang et al.[44], who observed protein structural unfolding (indicated by increased fluorescence intensity) induced by LAB fermentation. The relatively lower r values observed in the low-inoculum groups (1% and 3%) suggest that stronger hydrophobic interactions and residual aggregation persisted between protein molecules, indicating incomplete conformational unfolding.

3.8 Effect of inoculation level on the intrinsic fluorescence spectra of WEB

As shown in Figure 2D, all groups exhibited a significant intrinsic fluorescence emission peak near 340 nm, attributable to the fluorescence emission of aromatic residues in proteins, such as Trp, Tyr, and phenylalanine (Phe). The maximum emission peaks for both the WE and FWE groups were located in the 320–340 nm range, indicating that the fluorescence spectra of the system were predominantly contributed by Trp[45–46]. As the inoculum increased from 1% to 7%, the fluorescence emission peak underwent a slight red shift (from 330 to 335 nm), suggesting that the microenvironment of Trp residues became more polar. Protein unfolding induced by fermentation likely relocated Trp residues from hydrophobic cores to more hydrophilic surface regions. FWE-5% showed the highest fluorescence intensity, indicating the greatest degree of protein unfolding and the largest number of exposed Trp residues under this inoculation condition. In contrast, the fluorescence intensity of FWE-7% was lower than that of FWE-3% and FWE-5% (though still significantly higher than WE, $P < 0.05$). This suggests that an excessively high inoculum led to insufficient substrate concentration, limiting the ability of proteases to further expose Trp residues. Additionally, small peptides generated from excessive hydrolysis may have undergone re-aggregation or formed complexes with fermentation metabolites (e.g., organic acids, polyphenols), resulting in fluorescence quenching and a reduced quantum yield[47].

3.9 Effect of inoculation level on the surface hydrophobicity of WEB

As shown in Figure 2E, the surface hydrophobicity of all fermented whole egg (FWE) groups was significantly higher than that of the whole egg (WE) group (89.28 μg). The FWE-1% (104.21 μg) and FWE-7% (105.46 μg) groups showed the relatively higher values, with no significant difference between them ($P > 0.05$). This phenomenon was attributed to the profound conformational rearrangement of proteins during fermentation. The proteolytic system of LAB hydrolyzed peptide chains, thereby exposing originally buried hydrophobic amino acid residues (e.g., Leu, Phe, Ile) to the molecular surface[48]. Concurrently, organic acids produced by fermentation decreased the system pH to 4.0–4.5, near the protein isoelectric point. This reduced electrostatic repulsion and prompted the reorientation and surface exposure of hydrophobic regions[49]. The synergistic effect of proteolysis and acid-induced conformational changes collectively enhanced the surface hydrophobicity of the FWE system[50]. The increased exposure of Tyr residues and the observed fluorescence redshift further corroborated that fermentation promoted the unfolding of protein tertiary structures.

3.10 Effect of inoculation level on the FTIR spectra of WEB

FTIR spectra (Figure 3A) revealed the effect of fermentation on the secondary structure of proteins in the WEB. All samples showed a significant O–H stretching vibration absorption peak in the 3 400–3 500 cm^{-1} region. This peak reflected the hydrogen-bonding network of water molecules and protein hydroxyl groups. In the characteristic protein absorption region (1 500–1 700 cm^{-1}), the amide I band (1 600–1 700 cm^{-1}, primarily attributed to C=O stretching vibrations) and the amide II band (1 500–1 600 cm^{-1}, attributed to the coupling of C–N stretching and N–H bending vibrations) were clearly identifiable[51]. The amide I band peak positions for the FWE-5% and FWE-7% groups shifted slightly toward lower wavenumber. The amide I band is highly sensitive to the protein backbone vibrations and hydrogen-bonding network. This redshift was attributed to the reorganization of intermolecular hydrogen bonds induced by fermentation. The altered hydrogen-bonding pattern of peptide C=O groups lowers the vibrational energy level. This change occurs during the transition from α-helix to β-sheet or random coil structures[52]. Increased inoculation levels corresponded to a weakening of absorption peaks in the FTIR spectra. This indicated a reduction in the overall ordered protein structure, particularly in α-helix content. Fermentation-driven proteolytic hydrolysis disrupted the regular arrangement of the peptide backbone[53]. These spectral changes were consistent with the SDS-PAGE results. As the inoculation level increased, high-molecular-weight protein bands gradually disappeared, and low-molecular-weight bands intensified. This confirmed that proteins underwent a transition from an ordered to a looser conformation under enzymatic action. This structural loosening not only improved protein digestibility by increasing enzymatic accessibility but also exposed originally buried hydrophobic and aromatic amino acid residues to the molecular surface. This mechanism aligns with the observed increase in surface hydrophobicity and the changes in UV second-derivative spectra.

3.11 Effect of inoculation level on the CLSM images of WEB

CLSM images (Figure 3B) provided a direct visualization of the microstructural reconfiguration of the WEB induced by fermentation. The WE group exhibited dense red fat fluorescence spots with large particle sizes, while the green protein fluorescence was uniformly yet dispersedly distributed. This pattern reflected the natural, independent structural state of fat and native proteins. As the inoculation level increased from 1% to 3%, the number of fat fluorescence spots decreased, and their distribution became more

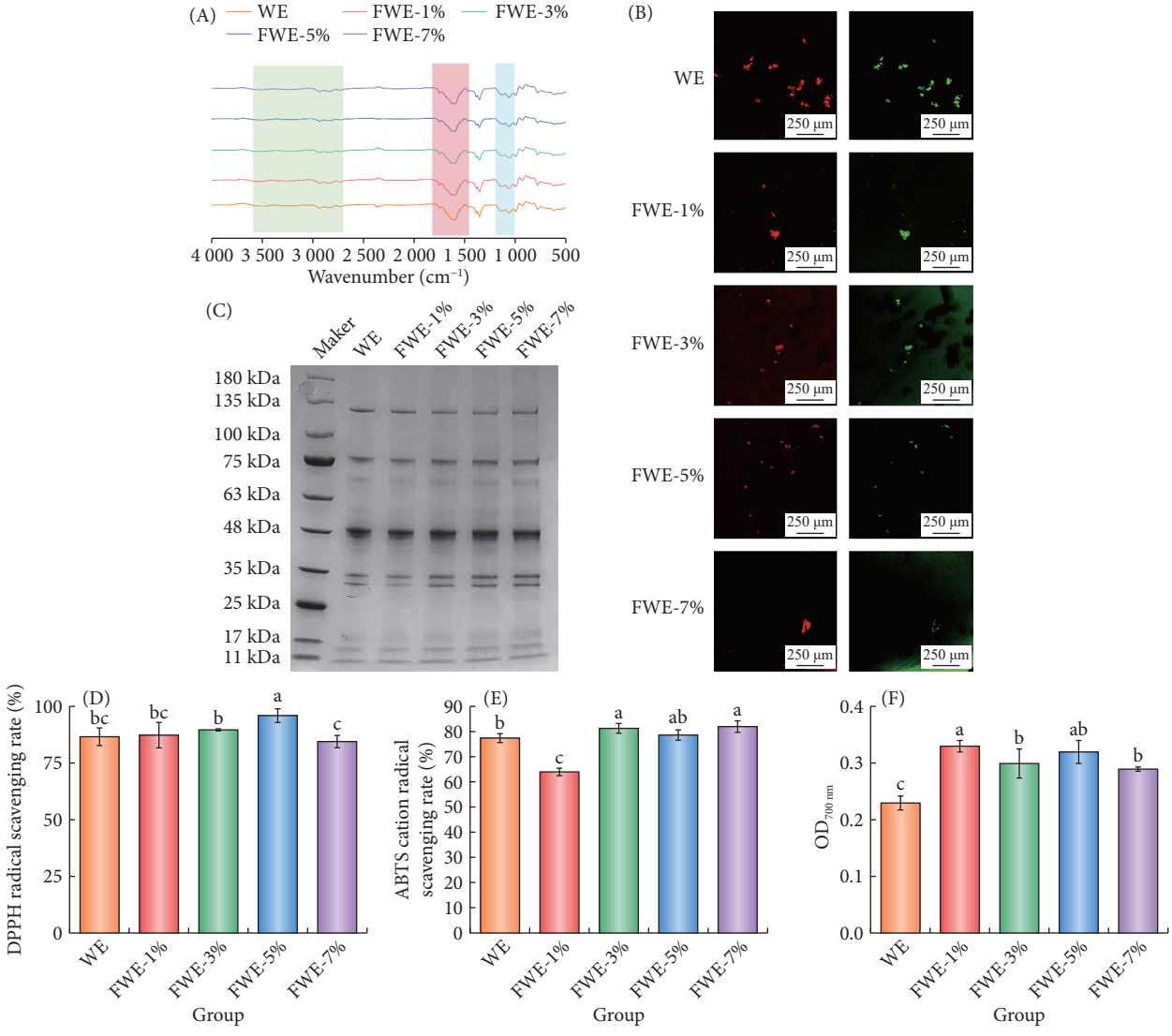

Figure 3 Effect of inoculation level on the (A) FTIR spectra, (B) CLSM images, (C) SDS-PAGE profiles, (D) DPPH radical scavenging activity, (E) ABTS cation radical scavenging activity and (F) FRAP of WEB. Different lowercase letters represent significant differences at $P < 0.05$.

homogeneous. Concurrently, the protein fluorescence intensified and gradually formed a network structure. This indicated that fat emulsification/dispersion and protein denaturation/cross-linking occurred simultaneously. This process led to the encapsulation of fat droplets[54]. The FWE-5% group presented the most typical structure, fat fluorescence was nearly absent. Intense and uniformly distributed protein fluorescence formed a dense three-dimensional emulsion gel network[23]. In contrast, although the FWE-7% group maintained a highly emulsified state, its protein network was excessively dense. This structural over-cross-linking may adversely affect the final product's texture[54]. In contrast, an excessively high inoculation level may impair the product texture. This impairment is due to structural over-compaction.

3.12 Effect of inoculation level on the SDS-PAGE profiles of WEB

The SDS-PAGE profile (Figure 3C) revealed the graded regulatory effect of fermentation on the subunit composition of whole egg proteins. All sample bands were primarily concentrated in the 48–110 kDa range. A band at approximately 48 kDa corresponded to major protein components such as ovalbumin. The unfermented whole egg (WE) group exhibited the most complete and intense high-molecular-weight (> 45 kDa) protein bands. In the FWE-1% group, the intensity of bands in this region slightly decreased, indicating the initial stage of proteolysis[44]. The FWE-3% group showed a significant reduction in band intensity. Band smearing was also observed. This suggested an accelerated hydrolysis phase. In the FWE-5% and FWE-7% groups, the high-molecular-weight protein bands were almost absent. This confirmed the thorough degradation of native proteins into low-molecular-weight fragments. In contrast, the intensity of low- and medium-molecular-weight protein bands (< 45 kDa) progressively increased with a higher inoculation level. A distinct new band appeared in the 30–35 kDa region for the FWE-3% group. The FWE-5% and FWE-7% groups showed very clear and dense band clusters in the region below 20 kDa. This verified the further breakdown of hydrolytic products into smaller peptides[55]. The extracellular proteases in the LAB system first degraded proteins into oligopeptides. These were subsequently hydrolyzed into low-molecular-weight peptides and amino acids by intracellular peptidases[56]. Concurrently, heat-induced conformational changes likely reduced the structural stability of the proteins, making them more susceptible to

enzymatic breakdown[57]. The stepwise increase in the inoculation level raised both microbial count and protease activity, thereby accelerating this cascade of hydrolysis. This systematic shift in subunit distribution toward lower molecular weights influences the rheological properties of the beverage. It may also significantly enhance its digestibility and reduce potential allergenicity[56].

3.13 Effect of inoculation level on the antioxidant activity of WEB

The DPPH radical scavenging activity showed an initial increase followed by a decrease with the inoculum level increased (Figure 3D). The DPPH radical scavenging activity of the FWE-5% group reached the peak value of 95.84%. In contrast, the FWE-7% group showed a significant decline to 84.24%. For ABTS cation radical scavenging activity (Figure 3E), the FWE-3%, FWE-5%, and FWE-7% groups recorded values of 81.21%, 78.70%, and 82.14%, respectively. All these values were higher than that of the WE group (77.59%). The ferric ion (Fe^{3+}) reducing capacity also increased with fermentation (Figure 3F). The FWE-1% and FWE-5% groups showed the higher $OD_{700\ nm}$ values (0.33 and 0.32, respectively). Under moderate inoculation (5%), microbial metabolism was highly active. Proteases effectively hydrolyzed the substrate. This process released low-molecular-weight bioactive peptides. These peptides were rich in hydrophobic amino acids, such as valine, leucine, and proline. Such peptides have been confirmed to possess the strongest radical scavenging capacity[58]. Conversely, an excessively high inoculation level (7%) intensified nutritional competition and caused a sharp pH drop in the early fermentation stage. The over-accumulation of metabolic by-products, such as organic acids and H_2O_2, inhibited the activity of key antioxidant enzymes. This led to the significant decrease in DPPH scavenging activity[59]. During fermentation, LAB produce various active substances, including peptides, organic acids, polyphenols, and flavonoids. These compounds collectively form the material basis for the antioxidant activity. A moderate inoculation level favors the sufficient generation of these substances. The metabolic inhibition effect caused by excessively rapid acid production at a high inoculation level was more pronounced in the DPPH and FRAP assays[60–61].

3.14 Effect of inoculation level on the IVPD of WEB

The results of simulated gastrointestinal digestion (Figure 4A) showed that the digestibility of the WE group was 81.0%. All fermented whole egg (FWE) groups showed increased digestibility. The increase varied in degree. The FWE-3% group had the highest digestibility at 84.9%. The FWE-1%, FWE-5%, and FWE-7% groups followed with values of 83.0%, 83.5%, and 83.6%, respectively. The lipids in egg yolk exist in the form of lipoprotein complexes. Their natural compact structure partially limits the accessibility of digestive enzymes[62]. During fermentation, LAB proteases and lipases cooperatively hydrolyzed these lipoprotein complexes. This partial degradation of apoprotein components (e.g., apovitellenin) exposed more enzymatic cleavage sites[63]. Simultaneously, the fermentation-induced rearrangement of protein secondary structures (consistent with FTIR spectra results) disrupted the native compact conformation. This made the substrate more accessible to digestive enzymes[64]. Additionally, the acidic environment may have promoted the partial dephosphorylation of phosvitin, further weakening its inherent resistance to digestion[65]. The optimal digestibility in the FWE-3% group may be attributed to the optimal metabolic activity of the microbiota under this condition. It produced a suitable amount of proteases and lipases without causing excessive protein hydrolysis or nutrient loss. An excessively high inoculation level (7%) likely led to over-acidification of the system. This could inhibit enzymatic activity or induce excessive protein aggregation, which was unfavorable for further improvement of digestion efficiency.

3.15 Effect of inoculation level on the GC-IMS of WEB

This study identified a total of 26 volatile compounds, comprising alcohols (6), esters (7), ketones (5), aldehydes (5), hydrocarbons (1), and pyrazines (2) (Table S1). The two-dimensional fingerprint plot (Figure 4B) and the differential topographic map (Figure 4C) visualize the distribution and intensity variation of volatiles across groups. Compared with the WE group, the FWE groups generated seven additional characteristic volatiles, namely 1-penten-3-ol, 2-methyl-1-propyl acetate, 2-heptanone, 3-hydroxy-2-butanone (acetoin), *n*-pentanal, 1-octene, and methylpyrazine (Figure 4D), whose formation can be mechanistically attributed to three synergistic pathways: i) LAB-driven central metabolism, which directly yields ketones, alcohols, and pyrazines, and promotes ester biosynthesis via intracellular esterases; ii) oxidative degradation of polyunsaturated fatty acids abundant in yolk phospholipids and milk fat, generating aldehydes, unsaturated alcohols, and alkenes; and iii) esterification between the hydrolysis-derived short-chain fatty acids and alcohols, enriching the ester profile[66–69]. PCA (Figure 4E) captured 89.03% of the total variance (PC1, 62.85%; PC2, 26.18%), with the WE group clearly separated from all FWE groups along PC1, reflecting a substantial shift in the volatile profile driven by fermentation-related organic-acid accumulation[70]. The tight clustering among FWE groups in the PC space suggests convergence of the core metabolite composition once fermentation has proceeded sufficiently, irrespective of inoculation level. The sensory contribution of each volatile, however, depends not only on its concentration but also on its odor threshold: low-threshold compounds such as 2-heptanone and 3-hydroxy-2-butanone exert strong flavor impact even at low concentrations, whereas high-threshold compounds such as 1-octene contribute marginally despite higher abundance[71]. The (*E*)-2-butenyl acetate, 1-propanol, and ethyl butyrate characteristic of the WE group constitute the original flavor baseline of the unfermented matrix; during fermentation, these precursors are preferentially metabolized or transformed by LAB intracellular/extracellular enzymes[72], leading to their marked reduction or disappearance. Among the fermentation-induced compounds, 3-hydroxy-2-butanone notably enhances the creamy-sweet note of the product; methylpyrazine, owing to its extremely low odor threshold, imparts the roasted-nutty and caramel-like aroma typical of thermally processed yolk lipids[73]; and benzaldehyde—derived from both lipid peroxidation and LAB-mediated transamination of Phe—contributes a characteristic almond note that further enriches the aromatic complexity of the fermented beverage[74].

3.16 Effect of inoculation level on the electronic nose response of WEB

Electronic nose PCA (Figure 5A) showed that PC1 (99.4%) and PC2 (0.31%) explained 99.71% of the variance. Substantial overlap

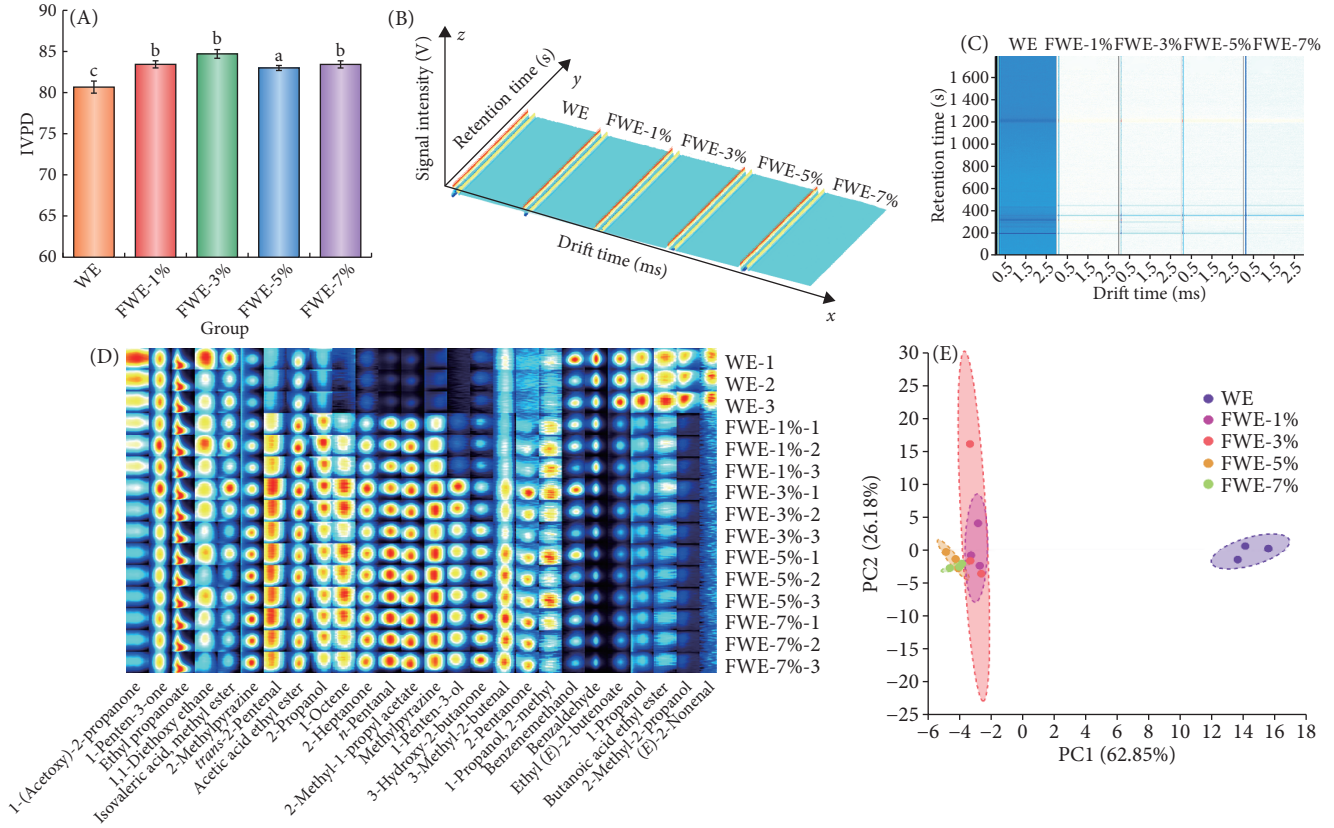

Figure 4 Effect of inoculation level on the (A) IVPD, (B) 3D topographic plots of GC-IMS, (C) 2D topographic plots of GC-IMS, (D) fingerprints of GC-IMS, and (E) PCA score plot of GC-IMS of WEB. Different lowercase letters represent significant differences at $P < 0.05$.

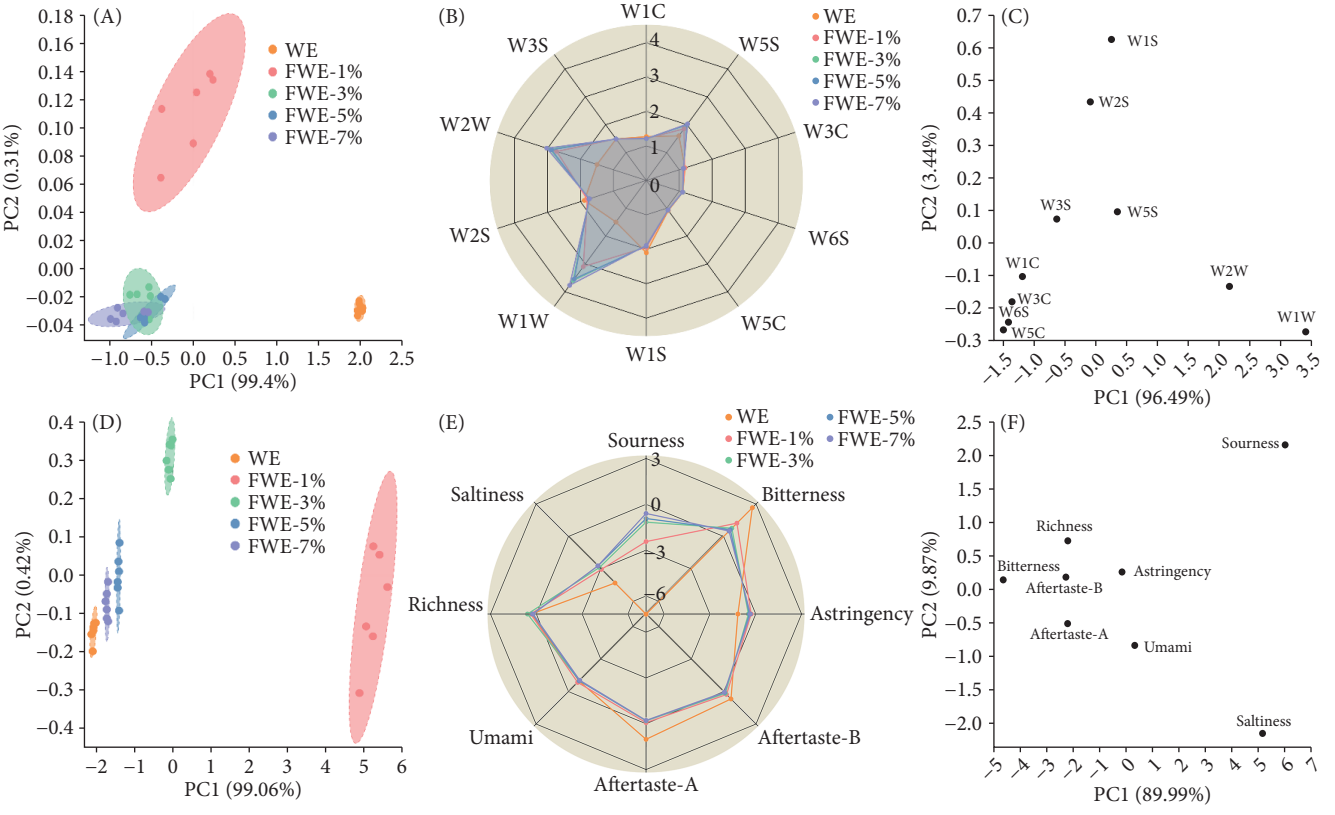

Figure 5 Effect of inoculation level on the (A) PCA score plot of electronic nose analysis, (B) radar chart of electronic nose components, (C) bioplot score plot of electronic nose analysis, (D) PCA score plot of electronic tongue analysis, (E) radar chart of electronic tongue components and (F) bioplot score plot of electronic tongue analysis of WEB.

was observed among FWE-3%, FWE-5%, and FWE-7%, which indicates similar aroma patterns for these groups. By contrast, WE and FWE-1% separated from the other samples, which suggests that fermentation intensity at low inoculation produced a distinct aroma profile. Sensor response analysis (Figure 5B) showed that sensors W1C, W3S, W3C, W6S, and W5C exhibited no significant changes among the groups. This suggests that the inoculation level had no significant effect on aromatic compounds and long-chain alkanes. The response values of sensors W1W, W2W, and W5S for the FWE-7% group were significantly higher than those for other groups. This indicates that fermentation increased the content of terpenes, nitrogen oxides, and sulfur-containing compounds in the WEB. Loadings analysis (Figure 5C) revealed that W1W and W1S contributed the most to PC1 and PC2, respectively. This means the odor differences in the fermented beverages were primarily driven by terpenes and methane derivatives[75]. During fermentation, LAB release enzymes such as transaminases and decarboxylases. These enzymes convert amino acids into aroma compounds like branched-chain aldehydes, alcohols, and carboxylic acids through transamination and decarboxylation reactions[40]. Simultaneously, lipids are broken down into free fatty acids by lipases. These fatty acids are then oxidized to generate volatile flavor substances such as alcohols, aldehydes, and acids. These combined metabolic pathways shape the distinctive aroma profile of the fermented WEB[76–77].

3.17 Effect of inoculation level on the electronic tongue response of WEB

In the PCA results from the electronic tongue analysis (Figure 5D), PC1 (99.06%) and PC2 (0.42%) together explained 99.48% of the total variance. The WE group clustered closely with the FWE-3%, FWE-5%, and FWE-7% groups in the PC space. This close clustering indicated that their taste profiles were similar, with no significant difference. In contrast, the FWE-1% group was significantly different from all other groups. The sensor radar chart (Figure 5E) showed that the sensors for sourness, saltiness, bitterness, astringency, and aftertaste had the most significant responses to the different groups. The responses for umami and richness were largely consistent across groups. Based on the evaluation of indices above the taste-less point (Figure 5E), the FWE-3% group showed the highest score for richness, which is associated with umami aftertaste. This result suggests that the FWE-3% group had the best mouthfeel. Sourness increased with a higher inoculation level. This increase resulted from the accumulation of organic acids produced during fermentation. These organic acids included lactic acid and acetic acid. The WE group had significantly lower saltiness and astringency but significantly higher bitterness than the FWE groups ($P < 0.05$). This indicated fermentation effectively reduced the content of bitter compounds[78]. The inoculation level had no obvious effect on the beverage's aftertaste. Saltiness and sourness contributed the most to PC1 and PC2, respectively (Figure 5F). This indicated that saltiness and sourness were the primary taste dimensions affected by the inoculation level in the fermented beverage. This is consistent with the radar chart results in Figure 5E. The catabolism by LAB significantly reduced the content of bitter amino acids in the WEB. The sourness of the fermented beverages increased significantly ($P < 0.05$). This increase indicated a reduction in the content of sweet amino acids. The FWE-3% group showed a significant increase in richness (umami aftertaste), meaning its content of umami amino acids was higher. Therefore, the optimal inoculation level was determined to be 3%.

3.18 Effect of inoculation level on the sensory evaluation of WEB

The sensory evaluation results (Figure 6A) showed that the WE group scored significantly lower than all FWE groups on all

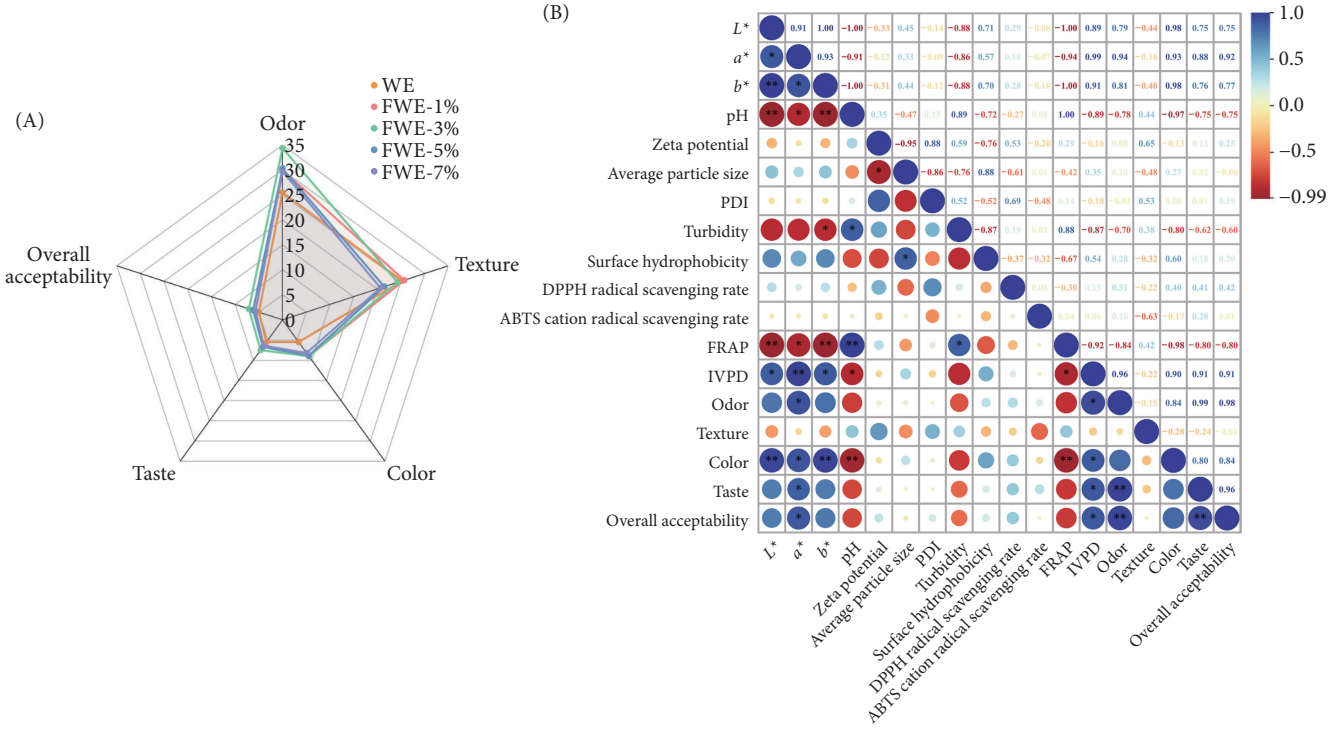

Figure 6 (A) Radar chart of sensory evaluation and (B) Pearson correlation heatmap among various indicators of WEB. * $P < 0.05$, ** $P < 0.01$.

attributes except texture. This confirmed that fermentation effectively improved the overall sensory quality of the WEB. The color scores were similar across groups (8–9), all presenting a light yellow hue. The scores for odor, taste, and overall acceptability initially increased and then decreased with higher inoculation levels, peaking at FWE-3%. Under this condition, the organic acids, amino acids, and volatile aroma compounds produced by fermentation were most balanced. This imparted a well-balanced sweet-sour taste, eliminated eggy odor, and created a mellow, smooth character to the beverage[79]. When the inoculation level increased to 5% and 7%, the sensory scores decreased significantly. This suggests that over-fermentation induced off-flavors or textural defects[80]. The trend for overall acceptability was consistent with the scores for individual attributes. This further verified that 3% was the optimal inoculation level. This result strongly aligned with the findings from the electronic tongue and electronic nose analyses. The electronic tongue indicated the highest richness for FWE-3%, and the electronic nose identified it as the comprehensively optimal group.

3.19 The correlation analysis among various indicators of WEB

The Pearson correlation heatmap (Figure 6B) systematically revealed the intrinsic relationships among physicochemical properties, sensory attributes, and functional activities under different inoculation levels. Color value showed a significant positive correlation with IVPD ($P < 0.05$). This suggests that the mild unfolding of proteins and microbial metabolites during fermentation may induce Maillard reactions or carotenoid release. Concurrently, the structural changes exposed cleavage sites for enzymes, synergistically promoting the improvement in digestibility[81]. pH was significantly positively correlated with turbidity and FRAP ($P < 0.05$). The pH reduction caused by fermentation was accompanied by protein aggregation. This aggregation led to increased turbidity. At the same time, the release of reductive amino acids or peptides enhanced the FRAP. Color value was significantly negatively correlated with FRAP and pH ($P < 0.05$). This shows that protein aggregation in the acidic environment increased turbidity while reducing color clarity[82]. Notably, sensory attributes (odor, color, taste) were all significantly negatively correlated with pH, turbidity, and FRAP ($P < 0.05$). This indicates that while a lower pH was beneficial for improving some antioxidant indicators, excessive acidification-induced protein aggregation and increased turbidity significantly impaired the product's appearance and taste[83].

4 Conclusion

This study systematically elucidated the dose-dependent effects of LAB inoculation level on the physicochemical properties, protein conformation, and flavor quality of fermented WEB. Fermentation improved appearance and dispersion uniformity (PDI of FWE-7% group decreased to 0.31) and enhanced antioxidant capacity (DPPH radical and ABTS cation radical scavenging rates reached 95.84% (FWE-5% group) and 82.14% (FWE-7% group), respectively). It also induced protein secondary-structure rearrangement and macromolecular degradation, thereby increasing protein bioaccessibility. Flavor profiling showed that 3% inoculation delivered the most favorable balance between aroma enrichment and suppression of eggy odor, consistent with the highest sensory scores. This work establishes a quantitative link between inoculation gradients and protein conformational evolution during WEB fermentation and strengthens mechanistic understanding of fermentation-driven structure-function relationships. Comprehensive quality characterization was achieved by integrating GC-IMS, electronic nose, and electronic tongue datasets. Further studies should clarify cholesterol metabolic dynamics during fermentation and validate the *in vivo* efficacy of fermentation-derived bioactive peptides; lipidomics and peptidomics are recommended, along with polysaccharide-protein composite strategies to enhance long-term colloidal stability. Overall, these findings provide a practical basis for precise process control and product development of egg-based functional fermented beverages.

Conflict of interest

The authors of this study have declared no conflict of interest.

Acknowledgements

This work was financially supported by the College Students Innovation Training Program of Shanxi Agricultural University (S202410113033) and the Shanxi Provincial General Program for Basic Research Project (202303021211093).

Author contributions

Danrong Yu: Conceptualization, data–acquisition, writing–original draft; Yaping Shen: Methodology, writing–original draft; Ni Zhang: Data–acquisition, editing–original draft; Yutong Han: Data–acquisition, editing–original draft; Bohan Wang: Data–acquisition, editing–original draft; Xiaoyu Zhang: Review & editing, data curation; Ling Ma: Conceptualization; Zhihui Yu: Formal analysis, supervision.

Appendix A. Supplementary data

Supplementary data associated with this article can be found, in the online version, at https://doi.org/10.26599/FSAP.2026.9240176.

References

[1] M. F. Medina-Cruz, D. Zárate-Contreras, R. V. Pérez-Ruiz, et al., Nutritional aspects, production and viability in the market of organic chicken eggs, Food Chem. Adv. 4 (2024) 100595. https://doi.org/10.1016/j.focha.2023.100595.

[2] Kashyap S, Shivakumar N, Varkey A, et al., Ileal digestibility of intrinsically labeled hen's egg and meat protein determined with the dual stable isotope tracer method in Indian adults, Am. J. Clin. Nutr. 108(5) (2018) 980–987. https://doi.org/10.1093/ajcn/nqy178.

[3] J. W. Kang, A. M. Zivkovic, Are eggs good again? A precision nutrition perspective on the effects of eggs on cardiovascular risk, taking into account plasma lipid profiles and TMAO, J. Nutr. Biochem. 100 (2022) 108906. https://doi.org/10.1016/j.jnutbio.2021.108906.

[4] Z. Li, Y. B. Song, Q. Y. Tang, et al., Effect of lactic acid bacteria fermentation on spray-dried egg yolk powder: powder characteristics, structural properties and gastrointestinal digestibility, IFSET 97 (2024) 103797. https://doi.org/10.1016/j.ifset.2024.103797.

[5] J. M. Miranda, X. Anton, C. Redondo-Valbuena, et al., Egg and egg-derived foods: effects on human health and use as functional foods, Nutrients 7(1) (2015) 706–729. https://doi.org/10.3390/nu7010706.

[6] Z. Q. Shang, D. R. Yu, J. J. Zhang, et al., Advances in research on the effects of lactic acid bacteria on the physicochemical, flavor, and nutritional characteristics of fermented egg products, Food Sci. Anim. Prod. 3(2) (2025) 9240112. https://doi.org/10.26599/FSAP.2025.9240112.

[7] Q. Zhang, X. J. Song, W. L. Sun, et al., Evaluation and application of different cholesterol-lowering lactic acid bacteria as potential meat starters, J. Food Prot. 84(1) (2021) 63–72. https://doi.org/10.4315/JFP-20-225.

[8] E. N. Asmaa, A. Ezzat, H. A. Farouk, et al., *Lactobacillus*-fermented yogurt exerts hypoglycemic, hypocholesterolemic, and anti-inflammatory activities in STZ-induced diabetic Wistar rats, Nutr. Res. 108 (2022) 22–32. https://doi.org/10.1016/j.nutres.2022.10.003.

[9] Y. Y. Liu, W. J. Kuang, M. Li, et al., Cholesterol-lowering mechanism of *Lactobacillus* bile salt hydrolase through regulation of *Bifidobacterium pseudolongum* in the gut microbiota, Nutrients 17(18) (2025) 3019. https://doi.org/10.3390/nu17183019.

[10] J. Jia, J. Y. Duan, X. Jia, et al., Mechanism of enhancing rehydration capacity and foaming property of spray-dried egg white powder by lactic acid fermentation, Food Hydrocoll. 153 (2024) 110037. https://doi.org/10.1016/j.foodhyd.2024.110037.

[11] Y. W. Jiang, J. Jia, D. D. Xiong, et al., Effects of short-term fermentation with lactic acid bacteria on egg white: characterization, rheological and foaming activities, Food Hydrocoll. 101 (2020) 105507. https://doi.org/10.1016/j.foodhyd.2019.105507.

[12] M. R. A. Porto, V. S. Okina, T. C. Pimentel, et al., Physicochemical stability, antioxidant activity, and acceptance of beet and orange mixed juice during refrigerated storage, Beverages 3(3) (2017) 36. https://doi.org/10.3390/beverages3030036.

[13] S. W. Yin, C. H. Tang, Q. B. Wen, et al., Conformational and thermal properties of phaseolin, the major storage protein of red kidney bean (*Phaseolus vulgaris* L.), J. Sci. Food Agric. 91(1) (2011) 94–99. https://doi.org/10.1002/jsfa.4155.

[14] N. Ahern, E. K. Arendt, A. W. Sahin, Protein soft drinks: a retail market analysis and selected product characterization, Beverages 9(3) (2023) 73. https://doi.org/10.3390/beverages9030073.

[15] D. Hueso, J. Fontecha, P. Gómez-Cortés, Comparative study of the most commonly used methods for total protein determination in milk of different species and their ultrafiltration products, Front. Nutr. 9 (2022) 925565. https://doi.org/10.3389/fnut.2022.925565.

[16] Z. H. Yu, J. R. Hu, S. X. Gao, et al., Joint effects of enzymatic and high-intensity ultrasonic on the emulsifying propertiesof egg yolk, Food Res. Int. 156 (2022) 111146. https://doi.org/10.1016/j.foodres.2022.111146.

[17] J. Y. Chen, K. S. Zhang, Y. X. Ren, et al., Influence of sodium tripolyphosphate coupled with (–)-epigallocatechin on the *in vitro* digestibility and emulsion gel properties of myofibrillar protein under oxidative stress, Food Funct. 11(7) (2020) 6407–6421. https://doi.org/10.1039/C9FO02361E.

[18] D. Zheng, D. R. Yu, S. Lin, et al., Enhancing salt-induced gelation of egg yolk granules through pH-ultrasound combined treatment: a physicochemical and microstructural analysis, Ultrason. Sonochem. 111 (2024) 107101. https://doi.org/10.1016/j.ultsonch.2024.107101.

[19] P. N. Anyiam, S. Phongthai, S. Sai-Ut, et al., Nutritional components and digestibility profiles of some potential plant-based protein sources, Foods 14(10) (2025) 1769. https://doi.org/10.3390/foods14101769.

[20] N. Loganayaki, P. Siddhuraju, S. Manian, Antioxidant activity and free radical scavenging capacity of phenolic extracts from *Helicteres isora* L. and *Ceiba pentandra* L., J. Food Sci. Technol. 50 (2013) 687–695. https://doi.org/10.1007/s13197-011-0389-x.

[21] A. Frontini, C. Negro, R. Accogli, et al., Valorization of a local Italian pear (*Pyrus communis* L. cv. 'Petrucina'), Foods 13(10) (2024) 1528. https://doi.org/10.3390/foods13101528.

[22] F. M. Elessawy, A. Vandenberg, A. El-Aneed, et al., An untargeted metabolomics approach for correlating pulse crop seed coat polyphenol profiles with antioxidant capacity and iron chelation ability, Molecules 26(13) (2021) 3833. https://doi.org/10.3390/molecules26133833.

[23] L. J. Yang, L. F. Wang, Y. J. Chi, Effect of whole egg liquid on physicochemical, quality, fermentation and sensory characteristics of yogurt, Foods 13(2) (2024) 321. https://doi.org/10.3390/foods13020321.

[24] U. Alvarado, J. Tacuri, A. Coloma, et al., Development of a hybrid system based on the CIELab colour space and artificial neural networks for monitoring pH and acidity during yogurt fermentation, Dairy 6(4) (2025) 41. https://doi.org/10.3390/dairy6040041.

[25] S. Leccese, A. Calcinoni, A. Wilson, et al., Orange carotenoid protein in mesoporous silica: a new system towards the development of colorimetric and fluorescent sensors for pH and temperature, Micromachines 14(10) (2023) 1871. https://doi.org/10.3390/mi1410187.

[26] T. Eilers, M. Legein, J. Temmermans, et al., Distribution of C_{30} carotenoid biosynthesis genes suggests habitat adaptation function in insect-adapted and nomadic Lactobacillaceae, Commun. Biol. 7(1) (2024) 1610. https://doi.org/10.1038/s42003-024-07291-2.

[27] L. Lopusiewicz, I. Dmytrów, A. Mituniewicz-Malek, et al., Natural gum from flaxseed by-product as a potential stabilizing and thickening agent for acid whey fermented beverages, Appl. Sci. 12(20) (2022) 10281. https://doi.org/10.3390/app122010281.

[28] M. L. Bulatović, T. Ž. Krunić, M. S. Vukašinović-Sekulić, et al., Quality attributes of a fermented whey-based beverage enriched with milk and a probiotic strain, RSC Adv. 4(98) (2014) 55503–55510. https://doi.org/10.1039/C4RA08905G.

[29] Y. Xie, Z. Y. Guan, S. T. Zhang, et al., Evaluation of sufu fermented using *Mucor racemosus* M2: biochemical, textural, structural and microbiological properties, Foods 12(8) (2023) 1706. https://doi.org/10.3390/foods12081706.

[30] A. Lazidis, R. D. Hancocks, F. Spyropoulos, et al., Whey protein fluid gels for the stabilisation of foams, Food Hydrocoll. 53 (2016) 209–217. https://doi.org/10.1016/j.foodhyd.2015.02.022.

[31] J. M. Li, S. P. Nie, The functional and nutritional aspects of hydrocolloids in foods, Food Hydrocoll. 53 (2016) 46–61. https://doi.org/10.1016/j.foodhyd.2015.01.035.

[32] A. K. Buggy, J. J. McManus, A. Brodkorb, et al., Pilot-scale formation of whey protein aggregates determine the stability of heat-treated whey protein solutions: effect of pH and protein concentration, J. Dairy Sci. 101(12) (2018) 10852–10864. https://doi.org/10.3168/jds.2017-14177.

[33] X. Y. Miao, H. H. Niu, M. Sun, et al., Structural characterization and properties of modified soybean meal protein via solid-state fermentation by *Bacillus subtilis*, Molecules 28(24) (2023) 8015. https://doi.org/10.3390/molecules28248015.

[34] A. M. Morris, M. A. Watzky, R. G. Finke, Protein aggregation kinetics, mechanism, and curve-fitting: a review of the literature, BBA 1794(3) (2009) 375–397. https://doi.org/10.1016/j.bbapap.2008.10.016.

[35] C. E. LaClair, M. R. Etzel, Turbidity and protein aggregation in whey protein beverages, J. Food Sci. 74(7) (2009) 526–535. https://doi.org/10.1111/j.1750-3841.2009.01260.x.

[36] X. H. Lü, H. B. Jin, X. Fu, et al., Egg white fermentation by lactic acid bacteria: effects on gel characteristics and preliminary investigation of suitable genera, Food Biosci. 61 (2024) 104582. https://doi.org/10.1016/j.fbio.2024.104582.

[37] S. Vargas-Díaz, H. J. Ciro-Velasquez, J. U. Sepúlveda-Valencia, Development and characterization of a fermented dairy beverage from permeated and concentrated sweet whey sweetened with tagatose, Rev. Fac. Nac. Agron. Medellín. 76(1) (2023) 10201–10212. https://doi.org/10.15446/rfnam.v76n1.100958.

[38] P. C. Imbachí-Narváez, J. U. Sepúlveda-Valencia, E. Rodriguez-Sandoval, Effect of modified cassava starch on the rheological and

quality properties of a dairy beverage prepared with sweet whey, Food Sci. Technol. 39(1) (2018) 134–142. https://doi.org/10.1590/1678-457X.28017.

[39] K. Phirom-On, A. Po-Ngern, S. Jaikhan, et al., Understanding the hindrance factor of bacterial proliferation and γ-aminobutyric acid-producing capability of nondairy strains of *Lactiplantibacillus plantarum* in milk fermentation, Sci. Rep. 13(1) (2023) 11464. https://doi.org/10.1038/s41598-023-38701-w.

[40] J. Jia, B. Ji, L. J. Tian, et al., Mechanism study on enhanced foaming properties of individual albumen proteins by *Lactobacillus* fermentation, Food Hydrocoll. 111 (2021) 106218. https://doi.org/10.1016/j.foodhyd.2020.106218.

[41] W. J. Jing, F. H. Hou, X. M. Wu, et al., A critical review on immobilized sucrose isomerase and cells for producing isomaltulose, Foods 13(8) (2024) 1228. https://doi.org/10.3390/foods13081228.

[42] Z. Xu, Z. X. Zhu, M. L. Tu, et al., Characterizations and the mechanism underlying cryoprotective activity of peptides from enzymatic hydrolysates of *Pseudosciaena crocea*, Foods 12(4) (2023) 875. https://doi.org/10.3390/foods12040875.

[43] Q. Chen, C. C. Che, J. F. Liu, et al., Construction of an exosome-functionalized graphene oxide based composite bionic smart drug delivery system and its anticancer activity, Nanotechnology 33(17) (2022) 175101. https://doi.org/10.1088/1361-6528/ac49bf.

[44] C. H. Chang, X. Y. Shen, W. Yi, et al., Lactic acid bacteria fermentation-induced egg white protein structure deformation influencing gelling properties, with membrane concentration as a strategy to improve texture, J. Food Sci. 89(11) (2024) 7083–7094. https://doi.org/10.1111/1750-3841.17327.

[45] A. B. Ghisaidoob, S. J. Chung, Intrinsic tryptophan fluorescence in the detection and analysis of proteins: a focus on Förster resonance energy transfer techniques, Int. J. Mol. Sci. 15(12) (2014) 22518–22538. https://doi.org/10.3390/ijms151222518.

[46] K. Ray, H. Szmacinsk, J. R. Lakowicz, Enhanced fluorescence of proteins and label-free bioassays using aluminum nanostructures, Anal. Chem. 81(15) (2009) 6049–6054. https://doi.org/10.1021/ac900263k.

[47] W. C. Ma, J. M. Wang, X. B. Xu, et al., Ultrasound treatment improved the physicochemical characteristics of cod protein and enhanced the stability of oil-in-water emulsion, Food Res. Int. 121 (2019) 247–256. https://doi.org/10.1016/j.foodres.2019.03.024.

[48] D. Muñoz-Provencio, G. Pérez-Martínez, V. Monedero, Characterization of a fibronectin-binding protein from *Lactobacillus casei* BL23, J. Appl. Microbiol. 108(3) (2010) 1050–1059. https://doi.org/10.1111/j.1365-2672.2009.04508.x.

[49] B. Çabuk, A. K. Stone, D. R. Korber, et al., Effect of *Lactobacillus plantarum* fermentation on the surface and functional properties of pea protein-enriched flour, Food Technol. Biotechnol. 56(3) (2018) 411. https://doi.org/10.17113/ftb.56.03.18.5449.

[50] T. Iwura, J. Fukuda, K. Yamazaki, et al., Conformational stability, reversibility and heat-induced aggregation of α-1-acid glycoprotein, J. Biochem. 156(6) (2014) 345–352. https://doi.org/10.1093/jb/mvu050.

[51] B. N. Gundogan, C. Saricoban, K. Unal, et al., The effect of different drying methods on some physico-chemical, functional and protein structure properties of liquid egg white fermented by *Lactobacillus rhamnosus* GG, J. Food Sci. Technol. 60(9) (2023) 2433–2443. https://doi.org/10.1007/s13197-023-05766-4.

[52] C. E. Guo, X. M. Guo, W. B. Chu, et al., Spectroscopic study of conformation changes of bovine serum albumin in aqueous environment, Chin. Chem. Lett. 30(6) (2019) 1302–1306. https://doi.org/10.1016/j.cclet.2019.02.023.

[53] O. S. Papadopoulou, A. A. Argyri, V. Kounani, et al., Use of Fourier transform infrared spectroscopy for monitoring the shelf life and safety of yogurts supplemented with a *Lactobacillus plantarum* strain with probiotic potential, Front. Microbiol. 12 (2021) 678356. https://doi.org/10.3389/fmicb.2021.678356.

[54] S. Hati, K. Ramanuj, S. Prakash, Influence of storage time of fermented soghurt on the changes in fat and protein biomolecules through confocal laser scanning microscopy (CLSM) under refrigeration condition, Discov. Food 4(1) (2024) 127. https://doi.org/10.1007/s44187-024-00214-4.

[55] J. Wang, L. L. Xu, Y. Q. Lü, et al., To improve the gel properties of liquid whole egg by short-term lactic acid bacteria fermentation, Innov. Food Sci. Emerg. Technol. 75 (2025) 102873. https://doi.org/10.1016/j.ifset.2021.102873,.

[56] S. Jain, A. K. Anal, Production and characterization of functional properties of protein hydrolysates from egg shell membranes by lactic acid bacteria fermentation, J. Food Sci. Technol. 54(5) (2017) 1062–1072. https://doi.org/10.1007/s13197-017-2530-y.

[57] Z. K. Wang, X. L. He, S. W. Wang, et al., Regulatory mechanism and flavor perception of heat induced conformational changes in chicken myofibrillar proteins on the binding affinity with sanshool and capsaicin, Food Chem. 495 (2025) 146594. https://doi.org/10.1016/j.foodchem.2025.146594.

[58] M. X. Jiang, K. Deng, C. L. Jiang, et al., Evaluation of the antioxidative, antibacterial, and anti-inflammatory effects of the aloe fermentation supernatant containing *Lactobacillus plantarum* HM218749.1, Mediat. Inflamm. 2016(1) (2016) 2945650. https://doi.org/10.1155/2016/2945650.

[59] Y. K. Wang, Q. M. Chen, Z. R. Lu, et al., Optimization of fermentation conditions for enhancing the antioxidant activity of medicine and food homologous materials using *Lactobacillus plantarum*, Lett. Appl. Microbiol. 78(4) (2025) 051. https://doi.org/10.1093/lambio/ovaf051.

[60] S. J. Li, Y. Tao, D. D. Li, et al., Fermentation of blueberry juices using autochthonous lactic acid bacteria isolated from fruit environment: fermentation characteristics and evolution of phenolic profiles, Chemosphere 276 (2021) 130090. https://doi.org/10.1016/j.chemosphere.2021.130090.

[61] M. Ghamry, A. F. Ghazal, Q. A. AI-Maqtqri, et al., Impact of a novel probiotic *Lactobacillus* strain isolated from the bee gut on GABA content, antioxidant activity, and potential cytotoxic activity against HT-29 cell line of rice bran, J. Food Sci. Technol. 59(8) (2022) 3031–3042. https://doi.org/10.1007/s13197-022-05512-2.

[62] J. H. Bie, W. D. Teng, Z. S. Peng, et al., Investigation on the physicochemical properties and volatile components of egg yolk fermented by different lactic acid bacteria and quality evaluation of mayonnaise prepared from fermented egg yolk, Food Biosci. 66 (2025) 106261. https://doi.org/10.1016/j.fbio.2025.106261.

[63] R. Mourad, I. Aljanabi, B. Csehi, et al., Simultaneous blending and fermentation of ToTu™ an egg-white drink with different fruit juices and probiotic lactic acid bacteria, Food Bioprod. Process. 150 (2025) 198–206. https://doi.org/10.1016/j.fbp.2025.01.008.

[64] Z. E. Tian, W. Q. Ge, J. J. Liu, et al., Improving the thermal fluidity of pasteurized egg white through lactic acid bacteria fermentation: rheological, structural, and functional characterizations, Food Chem. 30 (2026) 148228. https://doi.org/10.1016/j.foodchem.2026.148228.

[65] B. Yilmaz, D. Ağagündüz, Bioactivities of hen's egg yolk phosvitin and its functional phosphopeptides in food industry and health, J. Food Sci. 85(10) (2020) 2969–2976. https://doi.org/10.1111/1750-3841.15447.

[66] G. E. S. Molina, G. Ras, D. F. da Silva, et al., Metabolic insights of lactic acid bacteria in reducing off-flavors and antinutrients in plant-based fermented dairy alternatives, Compr. Rev. Food Sci. Food Saf. 24(2) (2025) 70134. https://doi.org/10.1111/1541-4337.70134.

[67] C. Chen, S. S. Zhao, G. F. Hao, et al., Role of lactic acid bacteria on the yogurt flavour: a review, Int. J. Food Prop. 20 (2017) 316–330. https://doi.org/10.1080/10942912.2017.1295988.

[68] X. Y. Yang, J. S. Xiao, P. Wan, et al., The effect of lutein on the oxidation of egg yolk phospholipids in a liposome model, Food Chem.: X 20 (2023) 100945. https://doi.org/10.1016/j.fochx.2023.100945.

[69] H. X. Tian, G. M. Zheng, H. Y. Yu, et al., Investigation of the interaction between lactones and ketones in a Cheddar cheese matrix using Feller's additive model, σ-τ plots, U-models, and aroma addition experiments, J. Dairy Sci. 107(8) (2024) 5496–5511. https://doi.org/10.3168/jds.2023-24339.

[70] X. Y. Wang, Y. Huang, B. Zhou, et al., Improvement of quality and flavor of salted egg yolks by ultrasonic assisted cooking, Ultrason. Sonochem. 75 (2021) 105579. https://doi.org/10.1016/j.ultsonch.2021.105579.

[71] S. Vatansever, B. Chen, C. Hall, Plant protein flavor chemistry fundamentals and techniques to mitigate undesirable flavors, Sustain. Food Proteins 2(1) (2024) 33–57. https://doi.org/10.1002/sfp2.1025.

[72] A. C. van Aalst, M. L. Jansen, R. Mans, et al., Quantification and mitigation of byproduct formation by low-glycerol-producing *Saccharomyces cerevisiae* strains containing Calvin-cycle enzymes, Biotechnol. Biofuels Bioprod. 16(1) (2023) 81. https://doi.org/10.1186/s13068-023-02329-9.

[73] M. X. Sun, L. Y. Ni, Y. H. Huang, et al., Effects of different drying treatments on the microstructure, free amino acids, volatile compounds and antioxidant activity of *Flammulina velutipes* root, Food Chem. 18 (2023) 100656. https://doi.org/10.1016/j.fochx.2023.100656.

[74] F. J. Hidalgo, R. Zamora, Formation of phenylacetic acid and benzaldehyde by degradation of phenylalanine in the presence of lipid hydroperoxides: new routes in the amino acid degradation pathways initiated by lipid oxidation products, Food Chem. 2 (2019) 100037. https://doi.org/10.1016/j.fochx.2019.100037.

[75] H. D. Zhang, H. X. Zhang, H. Du, et al., Unraveling the multiple interactions between phages, microbes and flavor in the fermentation of strong-flavor Baijiu, Bioresour. Bioprocess. 12(1) (2025) 14. https://doi.org/10.1186/s40643-025-00852-1.

[76] F. B. Siepmann, B. S. de Almeida, T. A. Gomes, et al., Biochemical, microbiological and technological characteristics of type II sourdoughs produced with lactic acid bacteria single-strains, Semina: Ciênc. Agrár. 43 (2022) 693–712. https://doi.org/10.5433/1679-0359.2022v43n2p693.

[77] T. Iizuka, T. Kagaya, K. Atsuda, et al., Evaluation of the taste of value added generic drugs by a taste sensor, J. Oral Tissue Eng. 9(3) (2012) 152–158. https://doi.org/10.11223/jarde.9.152.

[78] Y. J. Ruan, Y. R. Chen, J. Wang, et al., Lactic acid bacteria fermentation improves the physicochemical properties, bioactivity, and metabolic profiles of lychee pulp, Food Chem. 34 (2026) 103535. https://doi.org/10.1016/j.fochx.2026.103535.

[79] Z. Zhang, S. Guo, T. Wu, et al., Inoculum size of co-fermentative culture affects the sensory quality and volatile metabolome of fermented milk over storage, J. Dairy Sci. 105(7) (2022) 5654–5668. https://doi.org/10.3168/jds.2021-21733.

[80] D. Ghosh, P. C. Chattopadhyay, Application of principal component analysis (PCA) as a sensory assessment tool for fermented food products, J. Food Sci. Technol. 49(3) (2012) 328–334. https://doi.org/10.1007/s13197-011-0280-9.

[81] Y. Q. Pei, Z. Y. Deng, B. Li, Regulation on aggregation behavior and *in vitro* digestibility of phytic acid-whey protein isolate complexes: effects of heating, pH and phytic acid levels, Foods 13(21) (2024) 3491. https://doi.org/10.3390/foods13213491.

[82] B. O. Dereli, M. Türkyılmaz, M. Özkan, Clarification of pomegranate and strawberry juices: effects of various clarification agents on turbidity, anthocyanins, colour, phenolics and antioxidant activity, Food Chem. 413 (2023) 135672. https://doi.org/10.1016/j.foodchem.2023.135672.

[83] W. Wan, B. Xu, Development of an orange juice beverage formulated with oat β-glucan and whey protein isolate, J. Sci. Food Agric. 98(12) (2018) 4685–4691. https://doi.org/10.1002/jsfa.9002.